33rd Annual International Conference of the IEEE EMBS
Boston, Massachusetts USA, August 30 - September 3, 2011

Segmentation of Scarred and Non-Scarred Myocardium in LG Enhanced CMR Images using Intensity-Based Textural Analysis

Lasya Priya Kotu, Kjersti Engan, Trygve Eftestøl, Stein Ørn and Leik Woie

Abstract— **The Late Gadolinium (LG) enhancement in Cardiac Magnetic Resonance (CMR) imaging is used to increase the intensity of scarred area in myocardium for thorough examination. Automatic segmentation of scar is important because scar size is largely responsible in changing the size, shape and functioning of left ventricle and it is a preliminary step required in exploring the information present in scar. We have proposed a new technique to segment scar (infarct region) from non-scarred myocardium using intensity-based texture analysis. Our new technique uses dictionary-based texture features and dc-values to segment scarred and non-scarred myocardium using Maximum Likelihood Estimator (MLE) based Bayes classification. Texture analysis aided with intensity values gives better segmentation of scar from myocardium with high sensitivity and specificity values in comparison to manual segmentation by expert cardiologists.**

I. INTRODUCTION

Non-invasive estimation of cardiac pathology is gaining lot of importance lately. Post myocardial infarction, some patients will have reduced left ventricular ejection fraction (LVEF) as part of the myocardium will get scarred without functioning properly. With the help of recognized risk markers (LVEF and scar size), these patients are differentiated into patients with high and low risk of getting life threating irregular heart rhythms (ventricular arrhythmia). Patients with high risk of getting arrhythmia are inserted with Implantable Cardioverter-Defibrillator (ICD). An ICD is a small device that is placed in the patient's chest cavity to give electrical pulses or shocks to control ventricular arrhythmia condition. Today, the decision on who is getting ICD implantation is based mostly on LVEF. Hence, improved strategies are required for the identification of patients who benefit most from ICD beyond the recognized risk markers due to the following concerns: a) The ICD implantation procedure is expensive. b) Overall benefit of ICD implantation for the patients with low risk of arrhythmia is questionable. c) The Patients inserted with ICD can not undergo Cardiac Magnetic Resonance (CMR) imaging further.

Late Gadolinium (LG) enhanced CMR imaging is used to find the extent of damage occurred to the myocardium tissue post myocardial infarction. The use of contrast agents in CMR imaging helps in increasing the intensity of scarred tissue in myocardium for better examination. A study by Yan et al., shows that scarred area contains useful information that assists in finding the patients with high and low risk of arrhythmia [1]. There are manual and semi manual methods to classify scarred area from myocardium [1]. Automatic segmentation of scar tissue is important because scar size is largely responsible in ventricular remodeling [2]. Lot of attention is carried out for automatic segmentation of myocardium from the CMR images. Some previous publications have reported automatic segmentation of myocardium in late enhancement magnetic resonance images [3] , [4]. However, automatic segmentation of scar from the myocardium region is yet to be fully explored. Some earlier work carried out on segmenting scar from myocardium was reported in [4] and [5]. Support vector machine was used to classify scar (non-viable tissue) and myocardium (viable tissue) in delayed enhancement magnetic resonance images in [4]. In [5], infarct region is detected in CMR images obtained by Composite Strain Encoding (C-SENC) using a multi-stage method. However, these methods might not be suitable for differentiating high and low risk arrhythmia patients.

The main focus of this paper is to segment the scar tissue from myocardium tissue. This paper is a preliminary step in acquiring our ultimate task of distinguishing between patients with high and low risk of getting arrhythmia. The intensity level of scar is very high compared to myocardium in LG enhanced CMR images. But general thresholding schemes cannot be applied to CMR images as the intensity level varies within a scar, from slice to slice and from patient to patient. The results from our group's previous work [6] shows that there are textural differences between the healthy myocardium and the scar tissues. We used dictionary learning techniques and sparse representation to find textural features of both the regions. From our experiments we found that textural features alone are not enough to segment scar from myocardium. Hence, along with textural features, the intensity level of scar and myocardium is used as another feature in segmenting scar from myocardium. The methods and the material used in our work are described in the following section.

II. MATERIAL AND METHODS

CMR images from a group of 22 patients with high risk of arrhythmia and with implanted ICD were provided by the Department of Cardiology in Stavanger University Hospital. LG enhanced CMR images all of the 22 patients were obtained from 1.5 Tesla MRI machine using same protocol. These CMR images were stored according to the Digital imaging and communications in medicine (DICOM) format with 512×512 pixel resolution. The myocardium and scar

L. P. Kotu, K. Engan and T. Eftestøl are with The Department of Electrical Engineering and Computer Science, University of Stavanger, N-4036 Stavanger, Norway lasya.p.kotu@uis.no, kjersti.engan@uis.no

Leik Woie and Stein Ørn are with the Cardiology Department, Stavanger University Hostpital, Stavanger, Norway leikw@online.no

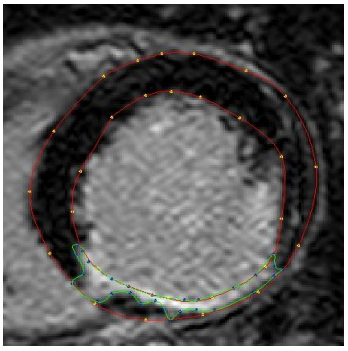

Fig. 1. Cropped short-axis CMR image showing manual segmentation of myocardium and scar tissues. The yellow and blue dots in the image are manually marked (by Cardiologist) coordinates to segment myocardium and scar. The red and green contours generated by cubic spline interpolations of the above coordinates show myocardium and scar tissues respectively.

tissue in all CMR images were segmented by an experienced cardiologist as shown in Fig. 1.

In this work we are looking at the capability of dictionary-based textural features combined with the dc-value of image patches for segmenting the scar tissue. Because of the obvious intensity differences in the healthy and scarred myocardium tissues in the LG enhanced CMR images, dc-value $dc(i,j)$ has been used as one of the features in a classifier. We define the feature $dc(i,j) = mean(I_{N\times N}(i,j))$ (where $I_{N\times N}$ is the neighborhood around the pixel $I(i,j)$), such that a new image I_{dc} , with $dc(i,j)$ as values at pixel position (i,j) is made as a sliding window averaging over the image. Dictionary learning and sparse representation are used to obtain the two textural features for each pixel in the image, one is correlated with textural features of healthy myocardial region $R_m(i,j)$ and the other one is correlated with textural features of scarred region $R_s(i,j)$. The features are combined to form the feature vector $x' = [R_s(i,j)\ R_m(i,j)\ dc(i,j)]$. These feature vectors are used in Maximum likelihood Estimator (MLE) based Bayes classifier to obtain the segmentation of scar tissue from myocardium. The dictionary-based textural features and Bayes classifier are described in the following sections.

III. DICTIONARY-BASED TEXTURAL FEATURES

In this paper, Recursive Least Squares Dictionary Learning Algorithm (RLS-DLA) presented in [7] is used for dictionary learning and Frame Texture Classification Method (FTCM) presented in [8] is used for sparse representation and texture classification. Sparse representations and learned dictionaries have been shown to work well for texture classification by Skretting and Husøy in [8] and by Mairal et al [9].

A dictionary D, is an ensemble of finite number of atoms which can be used for signal representation. A linear combination of some of the atoms in the dictionary gives an exact or approximate representation of the original signal. From the original CMR image, a $\sqrt{N}\times\sqrt{N}$ image patch is reorganized column wise into a column vector x of length N. We define a finite number of dictionary atoms of length N arranged as the columns in a matrix. The sparse representation $\tilde{x}$, or the approximation of the signal and the representation error r can be expressed as :

$$\tilde{x} = \sum_{k=1}^{K} w(k)d^{(k)} = Dw, \quad r = x - \tilde{x} = x - Dw, \qquad (1)$$

where K is the size of dictionary and w is the sparse coefficient vector. In a sparse representation only a small number of the coefficients $w(k)$ are allowed to be non-zero. Finding the sparse coefficient vector can be formulated as:

$$w = \underset{w}{argmin}\|w\|_0 + \gamma\|x - Dw\|_2^2 \qquad (2)$$

and is an NP-hard problem. This can be approximated by greedy methods or by changing the l_0 pseudo-norm by the l_1 norm. In this work, we used a greedy algorithm called Order Recursive Matching Pursuit (ORMP) algorithm [10].

Dictionary learning is the task of learning or training a dictionary on a available training set such that it adapts well to represent that specific class of signals. In this work, dictionaries were learned to represent scar and myocardium. The RLS-DLA presented in [7] is an on-line dictionary learning algorithm that updates the dictionary for every new training vector. RLS-DLA was used to train the dictionaries for myocardium and scar in our work. An interested reader can refer [7] for further details on RLS-DLA.

Frame Texture Classification Method (FTCM) introduced in [8] is observed closely as a supervised vector classification method. In FTCM, texture in a small image patch is modeled as sparse linear combination of dictionary atoms. Refer [8] for further details. The texture classification algorithm, FTCM used in our work proceeds as follows: Consider the myocardium in a CMR image I, that contains two texture classes: healthy and scarred myocardium. The training vector y_l for each pixel in the training image are made from that specific pixel and its neighborhood $N\times N$. In the training set, each pixel is classified into a specified texture class. Then, the dictionaries D_s and D_m are trained for the predefined texture classes (scar and myocardium) using RLS-DLA. Using the two trained dictionaries, each training vector y_l is then represented sparsely using ORMP vector selection algorithm [10]. For training and test sets, the residual images R_s and R_m which are of same size as the original image are calculated for the two texture classes. For each pixel in the myocardium of a training image, the residuals (or representation errors) calculated for healthy myocardium and scar dictionaries form the first two entries in the feature vector for MLE based Bayes classifier. The two residuals are calculated as:

$$R_s(i,j) = \|y_l - D_s w_l^s\| \text{ and } R_m(i,j) = \|y_l - D_m w_l^m\|, \qquad (3)$$

where w_l^s andw_l^m are sparse coefficient vectors.

IV. MAXIMUM LIKELIHOOD ESTIMATOR BASED BAYES CLASSIFICATION

The Maximum Likelihood(ML) [11] technique is a popular method for parametric estimation of an unknown probability density function(PDF). The ML estimates of the mean

m_{ML} and the covariance matrix S_{ML} of normally distributed data $X = \{x_1, x_2, \ldots, x_t, \ldots, x_N\}$ are given below:

$$m_{ML} = \frac{1}{N}\sum_{i=1}^{N} x_t \;\; and \;\; S_{ML} = \frac{1}{N}\sum_{i=1}^{N} (x_t - m_{ML})(x_t - m_{ML})^T, \tag{4}$$

where N is the number of training feature vectors. In this work, labeled feature vectors were formed for the two classes ω_c, $c = 1,2$: healthy myocardium and scar. The training feature vector used in our technique is framed as:

$$\begin{bmatrix} x_t \end{bmatrix} = \begin{bmatrix} R_s(i,j) \\ R_m(i,j) \\ dc(i,j) \end{bmatrix} = \begin{bmatrix} \|y_l - D_s w_l^s\| \\ \|y_l - D_m w_l^m\| \\ mean(I_{N\times N}(i,j)) \end{bmatrix}. \tag{5}$$

The test feature vectors are collected from the test image set, in the same way as training feature vectors. Before collecting test feature vectors for final segmentation, the test residual images are smoothed(using a $a \times a$ pixels separable Gaussian low pass filter with variance σ^2) because texture by definition is not a pixel by pixel phenomena [8]. Smoothing reduces overall segmentation error and improves the segmentation within the texture regions at the cost of increased segmentation error at the borders between various texture regions. Before smoothing the test residual images, a nonlinearity function can be applied on the residual images to improve texture segmentation as seen in [8]. Nonlinearity function can be either square root or inverse sine or logarithmic operation.

The training process involves calculating the ML estimates to find class specific $p(x|\omega_c)$, $c = 1,2$ and prior probabilities $P(\omega_c)$, $c = 1,2$. The Bayes decision theory is used to find the posterior probabilities $P(\omega_c|x) = p(x|\omega_c) * P(\omega_c)$ for the test feature vector. Bayes classifier assigns the test vector to the class that has greater posterior probability.

V. EXPERIMENT AND RESULTS

We performed experiments to segment scar from myocardium in CMR images using MLE based Bayes classifier with dictionary-based texture features and dc-values. All our experiments were carried out in MATLAB. CMR images from a group of 22 patients implanted with ICD were divided into training and testing groups with 15 and 7 patients respectively. The number of image slices with visible scar in each patient varies approximately from 5 to 12 depending on the size of scar and heart. Only short-axis image slices with visible scar were used in our experiments. The size of the scar varies from one slice to the other. As shown in Fig. 1 manual segmentation of myocardium and infarction areas were used as classification labels in our experiments. Preprocessing of any kind is not used on the images.

In all CMR Images, we take into account only myocardium segmented by cardiologists. Two sets of training vectors were generated from scar and healthy myocardium. The neighborhood size 5×5 was used to form training vectors as explained in III. The same neighborhood size must be used while training and finding residual images. Consider the pixels on the border zones, their neighborhood extends into other regions that are not under consideration. If we use training vectors from border regions, then the dictionaries might learn the texture properties of other regions along with the texture properties they are intended to learn. So, the training vectors for the pixels whose neighborhood span other regions were not considered in our experiments.This is depicted in Fig. 2. After generating the training vectors from both areas, the dictionaries were learned using RLS-DLA as explained in [7]. The dictionary size of 25×150 atoms was used in our experiments. Initial dictionaries were formed by randomly selecting 150 vectors of length 25 from the training sets.

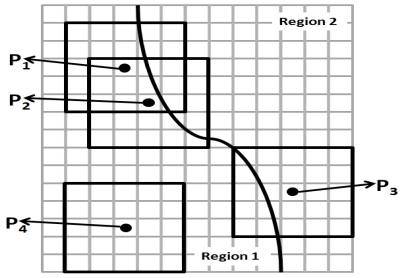

Fig. 2. Training vectors are generated from each pixel as long as that entire neighborhood lies within one texture region. The neighborhood of pixels P_1, P_2, P_3 includes more than one texture, and the corresponding feature vectors are excluded from the training set. P_4 has the entire neighborhood within one texture and hence the corresponding feature vector is included in that texture's training set.

After the training step, dictionaries were used on training and test images to obtain residual images as described in section III. Using 5×5 neighborhood, dc image I_{dc} were obtained as explained in II. For each pixel in the myocardium of training images, feature vectors were formed from residual and DC images as explained in sections II and III. We scaled the features to avoid dominance of one feature over the other. Dictionary-based texture features are correlated and hence they were jointly scaled to have zero mean and unit variance. DC-values were scaled separately to have zero mean and unit variance. The ML estimates of the labeled feature vector set were determined according to 4. The test feature vector set was calculated after including logarithmic nonlinearity and smoothing (using low pass Gaussian filter with $\sigma = 5$ and 9×9 window size) the test residual images. The scaling coefficients from the training were stored to scale the test vectors. The Bayes classifier assigns the test feature vector to the class that gives maximum posterior probability as discussed in previous section. Fig. 3 shows the results of segmentation of the scar from the myocardium using intensity-based texture analysis.

Sensitivity and specificity show the percent of correctly segmented scar and healthy myocardium tissues by our method in comparison to cardiologists segmentation. In table I, results in first and second column are from Bayes classifier with only dc-value and combination of dc-value and texture features respectively. Table I clearly shows that intensity-based texture analysis performs better and gives overall average sensitivity of 82.32% and specificity of 89.05%. Table I shows that dc-value alone is not sufficient

for better segmentation of scar.

For the test patients 2 and 3, our method works fairly well as the scar intensity assists better in segmentation. The performance of the method reduces in the test patients 6 and 7 as the intensity differentiation between scar and myocardium is minimal in these patients. It is also reflected in the first column of the table where only intensity value is used as a feature vector. Texture analysis combined with intensity values increases the sensitivity in patients 6 and 7. The test patient 4 is an outlier (intensity values are out of the typical range of other test patients) in our test set. Table I shows that the outlier is handled effectively by our method. Using automatic segmentation of myocardium instead of manual segmentation may improve our results further. Our results are comparable to the results reported (sensitivity of 81.34% and specificity of 92.28%) in [4]. We find it difficult to compare our results with [5] as it uses different approach for validation of results and CMR imaging technique.

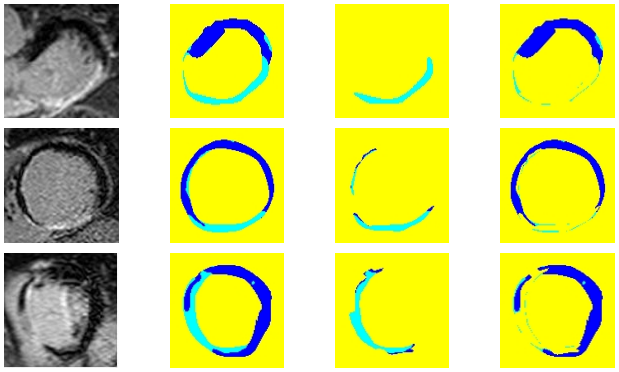

Fig. 3. Results of segmentation of scar and healthy myocardium on CMR images using intensity-based texture analysis. Column I: The cropped CMR images containing left ventricle. II: The manually segmented myocardium along with the segmentation results: blue - myocardium, cyan - scar, yellow - other image parts). III: Sensitivity: Segmented scar (cyan) in agreement with the manually segmented scar (blue). IV: Specificity: Healthy myocardium(blue) segmented as scar (cyan).

TABLE I

COMPARISON OF SENSITIVITY AND SPECIFICITY ON THE GROUP OF 7 TEST PATIENTS USING DC-VALUE dc AND INTENSITY-BASED TEXTURE ANALYSIS R_s, R_m, dc.

Sensitivity		
Test Patient	dc	R_s, R_m, dc
Patient 1	59,82	83,07
Patient 2	96,80	99,56
Patient 3	94,50	98,02
Patient 4	57,84	81,69
Patient 5	47,71	77,78
Patient 6	45,52	75,32
Patient 7	29,70	60,80
Average(SD)	61,70(25.1)	82,32(13.4)

Specificity		
Test Patient	dc	R_s, R_m, dc
Patient 1	99,62	98,65
Patient 2	86,22	67,12
Patient 3	93,53	88,04
Patient 4	97,48	94,60
Patient 5	95,45	89,34
Patient 6	98,25	94,49
Patient 7	95,86	91,08
Average(SD)	95,20(4,4)	89,05(10.3)

VI. CONCLUSION AND FUTURE WORK

A. Conclusion

In this paper, a new technique has been proposed to segment scar (infarct region) from healthy myocardium on LG enhanced CMR images using texture analysis by incorporating the knowledge of intensity variations in scar and healthy myocardium. In texture analysis, we have explored the learned dictionaries capability of capturing differences in the textures of scar and healthy myocardium. It is found that dictionary learning is capable of finding the textural differences even with a limited database of CMR images. The segmentation of scar and healthy myocardium tissue by intensity-based texture analysis is comparable to the manual segmentation by experts with sensitivity of 82.32% and specificity of 89.05%.

B. Future Work

We want to further explore our technique by using discriminant dictionary learning presented in [9]. In addition we are further exploring if the intensity-based texture analysis can be useful for separating high and low risk of arrhythmia patients to implant ICD for high risk arrhythmia patients.

REFERENCES

[1] A. Yan, A. Shayne, *et al.*, "Characterization of peri-infarct zone by contrast-enchanced cardiac magentic resonance imaging is a powerful predictor of post-myocardial infarction mortality," in *Pro. MICCAI 2004*, vol. 114. Circulation, 2006, pp. 32–39.

[2] S. Ørn, C. Manhenke, *et al.*, "Effect of left ventricular scar size, location, and transmurality on left ventricular remodeling with healed myocardial infarction," *The American Journal of Cardiology*, pp. 1109–1114, 2007.

[3] C. Ciofolo, M. Fradkin, and B. Mory, "Automatic myocardium segmentation in late-enhancement MRI," in *Symposium on Biomedical Imaging: From Nano to Macro, Paris, 2008.* IEEE, 2008, pp. 225 – 228.

[4] E. Dikici, T. O'Donnell, R. Setser, and R. White, "Quantification of delayed enchancement MR images," in *Pro. MICCAI 2004*, vol. 3216/ 2004. SpringerLink, 2004, pp. 250–257.

[5] A. O. Algohary, A. M. El-Bialy, *et al.*, "Detection of cardiac infarction in MRI C-SENC images," *Universal journal of Computer science engineering technology*, pp. 36–40, 2010.

[6] K. Engan, T. Eftestøl, S. Ørn, J. Kvaløy, and L. Woie, "Exploratory data analysis of image texture and statiscal features on myocardium and infarction areas in cardiac magnetic resonance images," in *Pro. EMBS 2010.* IEEE, 2010, pp. 5728–5731.

[7] K. Skretting and K. Engan, "Recursive least squares dictionary learning algorithm," in *Signal Processing*, vol. 58. IEEE, 2010, pp. 2121 – 2130.

[8] K. Skretting and J. Husøy, "Texture classification using sparse frame-based representations," *EURASIP on Applied Signal Processing*, 2006.

[9] J. Mairal, F. Bach, J. Ponce, G. Sapiro, and A. Zisserman, "Discriminative learned dictionaries for local image analysis," in *Pro. Computer Vision and Pattern Recognition, 2008.* IEEE, 2008, pp. 1–8.

[10] M. Gharavi-Alkhansari and T. Huang, "A fast orthogonal matching pursuit algorithm," in *Pro. ICASSP 1998.* IEEE, may 1998, pp. 1389–1392.

[11] S. Theodoridis and K. Koutroumbas, *Pattern Recognition*, 4th ed. Academic Press, 2008.